

BI-AXIAL PSEUDODYNAMIC TESTING

Gee-Yu LIU¹ And Shuenn-Yih CHANG²

SUMMARY

The bi-axial pseudodynamic technique is proposed for the testing of structures under two lateral perpendicular seismic excitations in this study. This technique consists of two major features. One is to manipulate large rigid body translations and rotation precisely, and the other is to update the restoring forces and torque experienced by the rigid specimen with respect to its moved configuration. These two features are achieved through a well-formulated scheme for configuration mapping, which takes into consideration the analytical geometrical relationships among the rigid specimen, the actuators and the reaction frames. The rigid body motion of the specimen can therefore be determined accurately from actuator lengths, and *vice versa*. As a consequence, the geometrically induced nonlinearity due to large rigid body motion in such kind of testing can be fully eliminated. Verification tests of: (1) a symmetric specimen under uni-axial seismic excitation; (2) a mass-eccentric and stiffness-symmetric specimen under bi-axial seismic excitation have both been conducted. Satisfactory experimental results fully support the feasibility of the proposed bi-axial pseudodynamic technique as a powerful vehicle for future research on seismic performances of large scale three-dimensional structures.

INTRODUCTION

In the past two decades, progress in theories and practices of pseudodynamic testing for research on structural dynamics has been made further and further. In addition, as major laboratories for large scale structural testing have been constructed around the world, the need of new pseudodynamic technique for three-dimensional structures instead of conventional two-dimensional planar structures emerges. Key issues of such non-planar technique had been fully studied and verification tests had been demonstrated [Thewalt and Mahin, 1995].

Three-dimensional structures like buildings (or bridge systems) usually consist of floors (or decks) of relatively high in-plane rigidity and supporting columns (or piers) of yet ordinary flexibility. Each floor (or deck) can, therefore, be considered as a rigid body with three degrees of freedom, two in translation and one in rotation. If the vertical components of excitation and response of either floors (or decks) or supporting columns (or piers) can be neglected, the technique interested here will be the control of motion of a flexibly-supported rigid specimen in Axes X and Y, and can be denoted as "bi-axial" technique. In this study, a novel bi-axial pseudodynamic technique is proposed for the testing of such structures under two lateral perpendicular seismic excitations.

To consider the setup of such testing geometrically, it can be observed that all employed actuators have two swivels: one is mounted on the specimen, the other on the reaction frame. The ones on the specimen can be regarded as parts of the specimen and will move together with the specimen as a rigid body. Let the centers (of rotation) of these swivels be denoted as $A, B, C \dots$ While the others on the reaction frame(s) can be regarded as fixed in the space, and the corresponding swivel centers can be denoted as $O, P, Q \dots$ Fig.(1) depicts

¹ National Center for Research on Earthquake Engineering, Taipei, Taiwan, Email : karl@email.ncee.gov.tw

² National Center for Research on Earthquake Engineering, Taipei, Taiwan, Email : sychang@email.ncee.gov.tw

schematically the geometry of the present case. Consequently, the motion of the rigid specimen can be described by Points $A', B', C' \dots$ (the moved positions of $A, B, C \dots$), and can be determined by the lengths of Segments $OA', PB', QC' \dots$ (the corresponding lengths of actuators).

RIGID BODY MOTION

The planar motion of a rigid body consists of three degrees of freedom, two in translation and one in rotation. Let these degrees of freedom be denoted as (X, Y) and Θ . Then, the equations of motion governing such a rigid body as a dissipated dynamic system under two lateral perpendicular seismic excitations can be expressed as:

$$\begin{aligned} M \cdot \ddot{X} + C_X \cdot \dot{X} + K_X \cdot X &= f_X(t) = M \cdot \ddot{g}_X(t) \\ M \cdot \ddot{Y} + C_Y \cdot \dot{Y} + K_Y \cdot Y &= f_Y(t) = M \cdot \ddot{g}_Y(t) \\ I_E \cdot \ddot{\Theta} + C_\Theta \cdot \dot{\Theta} + K_\Theta \cdot \Theta &= f_\Theta(t) = 0 \end{aligned} \quad (1)$$

where M and I_E are the mass and the moment of inertia of the rigid body with respect to its center of mass E , respectively. C_* , K_* , and $f_*(t)$ ($*$ = X, Y, Θ) denote the damping, stiffness, and seismic excitation terms, respectively. $\ddot{g}_X(t)$ and $\ddot{g}_Y(t)$ are the two ground accelerations interested. The dot means derivative with respect to time t .

During the pseudodynamic procedure, the restoring forces (torque) $K_X \cdot X$, $K_Y \cdot Y$, and $K_\Theta \cdot \Theta$ will be replaced by the resultants F_X and F_Y in X and Y , and by torque T_E with respect to Point E . Since the testing will be under quasi-static condition, resultants F_X , F_Y and torque T_E are supposed to be calculable from the feedback readings of the actuator forces.

GEOMETRICAL MAPPINGS

During the bi-axial pseudodynamic procedure, at times the lengths of actuators have to be determined and the corresponding strokes to be executed after the target motion of the rigid specimen being calculated. Also, the measured motion of the rigid specimen has to be determined after the feedback of actuator stroke readings. In this section, a step-by-step description on the geometrical mappings between the motion of the rigid specimen and the actuator lengths in the moved configuration will be shown. It should be noted that three is the least number of actuators for full control of a rigid body in planar motion. In the following formulation, the considered rigid specimen will be attached with and controlled by four actuators. Cases with more than four actuators (for reasons of, says, higher load capacity) can be easily extended.

Let $ABCD$ (or ΔABC , if only three actuators are used) be the initial configuration of the rigid specimen, $A'B'C'D'$ (or $\Delta A'B'C'$) be the corresponding moved configuration, and Points E and E' be the centers of mass of the two configurations, respectively. Note that the shape of $A'B'C'D'$ (or $\Delta A'B'C'$) will always be identical to the shape of $ABCD$ (or ΔABC). Define $b = AB$, $c = AC$, $d = AD$, $e = AE$, $\psi_c = \angle CAB$, $\psi_d = \angle DAB$ and $\psi_e = \angle EAB$. All these are constant geometrical measures of the geometry of the rigid body.

Define θ , ϕ , ϕ_b , ϕ_c , ϕ_d as the angles between Axis X and the vectors \overline{AB} , \overline{OA} , \overline{PB} , \overline{QC} , \overline{RD} , respectively. Also, define r_a , r_b , r_c and r_d as the initial lengths of the actuators (swivel center-to-center lengths, to be precise). All these symbols superscripted with prime will be used to denote their counterparts in the moved configuration. Obviously, the rigid body translation and rotation can be expressed by $(X, Y) = EE'$ and $\Theta = \theta' - \theta$.

Find the target lengths r_a' , r_b' , r_c' and r_d' from (X, Y) and Θ .

Step I. Calculate vectors $\overline{OA} \sim \overline{OE}$ according to the initial configuration as:

$$\begin{aligned}
\overrightarrow{OA} &= (r_a \cos \phi, r_a \sin \phi) \\
\overrightarrow{OB} &= (r_a \cos \phi + b \cos \theta, r_a \sin \phi + b \sin \theta) \\
\overrightarrow{OC} &= (r_a \cos \phi + c \cos(\theta + \psi_c), r_a \sin \phi + c \sin(\theta + \psi_c)) \\
\overrightarrow{OD} &= (r_a \cos \phi + d \cos(\theta + \psi_d), r_a \sin \phi + d \sin(\theta + \psi_d)) \\
\overrightarrow{OE} &= (r_a \cos \phi + e \cos(\theta + \psi_e), r_a \sin \phi + e \sin(\theta + \psi_e))
\end{aligned} \tag{2}$$

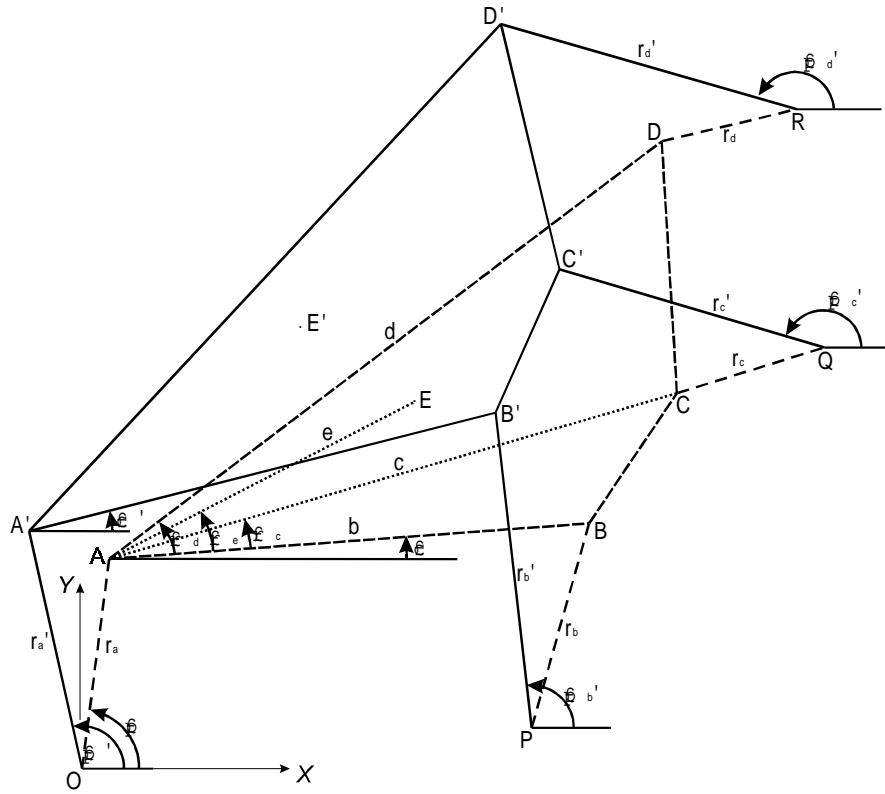


Figure 1: Geometry of a rigid specimen and actuators.

Then, calculate vectors $\overrightarrow{EA} \sim \overrightarrow{ED}$ as:

$$\begin{aligned}
\overrightarrow{EA} &= \overrightarrow{OA} - \overrightarrow{OE} = (-e \cos(\theta + \psi_e), -e \sin(\theta + \psi_e)) \\
\overrightarrow{EB} &= \overrightarrow{OB} - \overrightarrow{OE} = (b \cos \theta - e \cos(\theta + \psi_e), b \sin \theta - e \sin(\theta + \psi_e)) \\
\overrightarrow{EC} &= \overrightarrow{OC} - \overrightarrow{OE} = (c \cos(\theta + \psi_c) - e \cos(\theta + \psi_e), c \sin(\theta + \psi_c) - e \sin(\theta + \psi_e)) \\
\overrightarrow{ED} &= \overrightarrow{OD} - \overrightarrow{OE} = (d \cos(\theta + \psi_d) - e \cos(\theta + \psi_e), d \sin(\theta + \psi_d) - e \sin(\theta + \psi_e))
\end{aligned} \tag{3}$$

Step II. Calculate:

$$\begin{aligned}
\overrightarrow{OA'} &= \overrightarrow{OE} + \overrightarrow{EE'} + \overrightarrow{E'A'} \\
\overrightarrow{OB'} &= \overrightarrow{OE} + \overrightarrow{EE'} + \overrightarrow{E'B'} \\
\overrightarrow{OC'} &= \overrightarrow{OE} + \overrightarrow{EE'} + \overrightarrow{E'C'} \\
\overrightarrow{OD'} &= \overrightarrow{OE} + \overrightarrow{EE'} + \overrightarrow{E'D'}
\end{aligned} \tag{4}$$

where $\overrightarrow{E'A'} = [T] \cdot \overrightarrow{EA}$, $\overrightarrow{E'B'} = [T] \cdot \overrightarrow{EB}$, $\overrightarrow{E'C'} = [T] \cdot \overrightarrow{EC}$, $\overrightarrow{E'D'} = [T] \cdot \overrightarrow{ED}$, and $[T] = \begin{bmatrix} \cos \Theta & -\sin \Theta \\ \sin \Theta & \cos \Theta \end{bmatrix}$. All are constants except $\overrightarrow{EE'} = (X, Y)$ and $[T] = [T(\Theta)]$, which are the rigid body translation vector and the rotation matrix.

Step III. Calculate the target lengths of actuators r_a' , r_b' , r_c' and r_d' as:

$$r_a' = |\overrightarrow{OA'}|, r_b' = |\overrightarrow{OB'} - \overrightarrow{OP}|, r_c' = |\overrightarrow{OC'} - \overrightarrow{OQ}|, r_d' = |\overrightarrow{OD'} - \overrightarrow{OR}| \quad (5)$$

Find (X, Y) and Θ from the measured actuator lengths r_a' , r_b' , r_c' and r_d' .

Step I. Assume an arbitrary set of (X^v, Y^v) and Θ^0 as the unknown rigid body motion of the moved configuration. Calculate the corresponding actuator lengths r_a^v , r_b^v , r_c^v and r_d^v through the steps in the previous sub-section.

Step II. Try to create a “cost function”, of which the functional value can be served as a measure of how (X^0, Y^0) and Θ^0 are close to the actual rigid body motion. One possible candidate for such purpose may be

$$f(X^0, Y^0, \Theta^0) = |r_a' - r_a^0|^2 + |r_b' - r_b^0|^2 + |r_c' - r_c^0|^2 + |r_d' - r_d^0|^2 \quad (6)$$

Obviously, the smaller the value of the cost function is, the closer the values of the variables (X^v, Y^v) and Θ^0 are to give the actual moved configuration of the rigid specimen. Note that the form of feasible cost functions is not unique. Eq.(6) will be employed throughout this study.

Step III. Find the values of (X^*, Y^*) and Θ^* for the variables (X^v, Y^v) and Θ^0 which can minimize the cost function in Step II most. Accept these values for the actual rigid body motion corresponding to the measured r_a' , r_b' , r_c' and r_d' .

An effective option to the present optimization case is the so-called “Simplex Method” [Press *et al.*, 1992]. In this study, it is found that quick and accurate search of (X^*, Y^*) and Θ^* is always guaranteed if each search is started with the values of (X, Y) and Θ at the previous time step.

After (X^*, Y^*) and Θ^* are found, calculate the angle ϕ' from the direction cosine of vectors OA' , whose expression is given in Eq.(4). Also, calculate $\theta' = \theta + \Theta^*$.

RESTORING FORCES AND TORQUE

Let F_a' , F_b' , F_c' , F_d' be the measured forces of the actuators along OA' , PB' , QC' and RD' . Then, the restoring forces (F_X, F_Y) and torque T_E experienced by the rigid specimen can be calculated through the following steps.

Step I. Calculate angles ϕ_b' , ϕ_c' , ϕ_d' from the direction cosines of vectors $\overrightarrow{PB'}$, $\overrightarrow{QC'}$, and $\overrightarrow{RD'}$ as:

$$\begin{aligned} \overrightarrow{PB'} &= \overrightarrow{OA'} + \overrightarrow{AB'} - \overrightarrow{OP} = (r_a' \cos \phi' + b \cos \theta' - P_x, r_a' \sin \phi' + b \sin \theta' - P_y) \\ \overrightarrow{QC'} &= \overrightarrow{OA'} + \overrightarrow{AC'} - \overrightarrow{OQ} = (r_a' \cos \phi' + c \cos(\theta' + \psi_c) - Q_x, r_a' \sin \phi' + c \sin(\theta' + \psi_c) - Q_y) \\ \overrightarrow{RD'} &= \overrightarrow{OA'} + \overrightarrow{AD'} - \overrightarrow{OR} = (r_a' \cos \phi' + d \cos(\theta' + \psi_d) - R_x, r_a' \sin \phi' + d \sin(\theta' + \psi_d) - R_y) \end{aligned} \quad (7)$$

where ϕ' and θ' have been determined at the end of the previous sub-section

Step II. Calculate the following vectors:

$$\begin{aligned}
\overrightarrow{E'A'} &= (-e \cos(\theta'+\psi_e), -e \sin(\theta'+\psi_e)) \\
\overrightarrow{E'B'} &= \overrightarrow{A'B'} + \overrightarrow{E'A'} = (b \cos \theta' - e \cos(\theta'+\psi_e), b \sin \theta' - e \sin(\theta'+\psi_e)) \\
\overrightarrow{E'C'} &= \overrightarrow{A'C'} + \overrightarrow{E'A'} = (c \cos(\theta'+\psi_c) - e \cos(\theta'+\psi_e), c \sin(\theta'+\psi_c) - e \sin(\theta'+\psi_e)) \\
\overrightarrow{E'D'} &= \overrightarrow{A'D'} + \overrightarrow{E'A'} = (d \cos(\theta'+\psi_d) - e \cos(\theta'+\psi_e), d \sin(\theta'+\psi_d) - e \sin(\theta'+\psi_e))
\end{aligned} \tag{8}$$

Step III. Calculate the restoring forces as:

$$\begin{aligned}
F_X &= F_a' \cos \phi' + F_b' \cos \phi_b' + F_c' \cos \phi_c' + F_d' \cos \phi_d' \\
F_Y &= F_a' \sin \phi' + F_b' \sin \phi_b' + F_c' \sin \phi_c' + F_d' \sin \phi_d'
\end{aligned} \tag{9}$$

and the torque with respect to Point E' as:

$$\begin{aligned}
(0, 0, T_E) &= \overrightarrow{E'A'} \times F_a' (-\cos \phi', -\sin \phi', 0) + \overrightarrow{E'B'} \times F_b' (-\cos \phi_b', -\sin \phi_b', 0) \\
&+ \overrightarrow{E'C'} \times F_c' (-\cos \phi_c', -\sin \phi_c', 0) + \overrightarrow{E'D'} \times F_d' (-\cos \phi_d', -\sin \phi_d', 0)
\end{aligned} \tag{10}$$

Eq.(10) can further be reduced to:

$$\begin{aligned}
T_E &= F_a' e \sin(\theta'+\psi_e - \phi') + F_b' \{e \sin(\theta'+\psi_e - \phi_b') - b \sin(\theta' - \phi_b')\} \\
&+ F_c' \{e \sin(\theta'+\psi_e - \phi_c') - c \sin(\theta'+\psi_c - \phi_c')\} + F_d' \{e \sin(\theta'+\psi_e - \phi_d') - d \sin(\theta'+\psi_d - \phi_d')\}
\end{aligned} \tag{11}$$

VERIFICATION TESTS

Test Setup

In the verification tests, a 2500mm×2500mm×400mm RC block, which was mounted symmetrically on four steel columns with identical cross section of H100×100×6×8 and length of 2780mm, was served as the flexibly supported rigid specimen. Three actuators of the MTS 243.70 single-ended static type were employed. The MTS FlexTest IIm control system was also used as the hydraulic servo controller. The columns were arranged such that their centers of cross-sections were located at the vertexes of a 2m×2m square. All major axes of these columns were aligned along the Y direction. The setup of the testing is depicted in Fig.(2) and will be served as the initial configuration.

Test Results

Firstly, consider the symmetric specimen under uni-axial seismic excitation in the X direction. The N-S component of the El Centro earthquake record with its peak ground acceleration scaled to 0.2g was used. The dynamic parameters of the considered dynamic system are listed in Tab.(1). Both the pseudodynamic response (dotted line) and the simulated response (solid line) of the rigid specimen are depicted in Fig.(3). The well-known Newmark explicit algorithm was employed as the integration scheme.

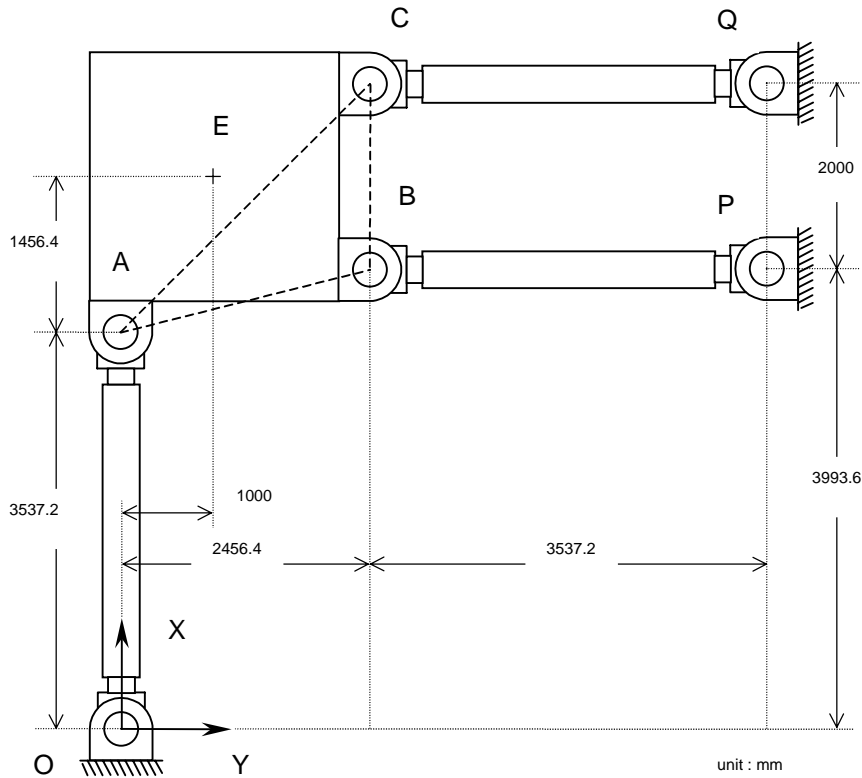


Figure 2: Schematic diagram of the bi-axial pseudodynamic testing setup.

Table 1: Dynamic parameters of the specimen.

Inertia terms	$M = 6,760Kg$	$I_E = 7,042Kg \cdot m^2$	
Damping terms	$C_X = 2.5 \times 10^3 N \cdot s / m$	$C_Y = 8.0 \times 10^3 N \cdot s / m$	$C_\Theta = 8.0 \times 10^5 N \cdot m \cdot s / rad$
Stiffness terms	$K_X = 1.346 \times 10^6 N / m$	$K_Y = 0.464 \times 10^6 N / m$	$K_\Theta = 1.810 \times 10^6 N \cdot m / rad$

It is seen that, along the direction of excitation, the pseudodynamic response matches very well with the simulated response. Yet for both the Y and Θ components of motion, the pseudodynamic response drifts instead of keeping fixed to zero. Parts of the reasons are that the stiffness of the supporting columns is too small, and that the specimen was not perfectly aligned to Axes X and Y .

It should be pointed out that under the current setup, it is very difficult to control accurately the motion of the rigid specimen along Axis Y while change in Θ is not significant. This is due to the fact that presently Actuator OA was aligned at the edge instead of the center of the specimen, and consequently the control of motion in Axis Y requires the assistance of both Actuators PB and QC . Since a small amount of displacement in the Y direction will need a much smaller length change in both Actuators PB and QC , which might be too small to compare with the precision of the built-in LVDTs in the actuators. As a result, the control over the Y component will be lost. This also leads directly to the inaccuracy in both the Y and Θ components of the pseudodynamic response.

In order to take into consideration the case of mass eccentricity, an offset of $(0.5m, -0.5m)$ to Point E was applied on purpose to create such effect artificially, and the moment of inertia had been arbitrarily modified as $I_E = 20,562Kg \cdot m^2$. For testing of the specimen under bi-axial seismic excitation, the N-S and E-W components of the El Centro earthquake record were used for excitation in the X and Y directions, respectively. Both the peak ground accelerations were scaled to $0.1g$. Fig.(4) depicts the responses of the specimen from the

pseudodynamic testing (dotted line) and from simulation (solid line). As in the previous case, both the Y and Θ components of the pseudodynamic response drifts again. However, the dynamic responses from both the pseudodynamic testing and simulation match in amplitude as well as in phase to some degree.

CONCLUSION

The proposed bi-axial pseudodynamic technique has been developed and implemented successfully. A configuration-mapping scheme, which employs the analytical geometrical relationships among the rigid specimen, the actuators, and the reaction frames, has been well formulated for the calculation of the rigid body motion of the specimen from actuator lengths and *vice versa*. As a consequence, the geometrically induced nonlinearity due to large rigid body motion in such kind of testing can be fully eliminated. In addition, since the theoretical rigidity of the floors (or decks) can be guaranteed *via* the configuration-mapping scheme, the specimen won't have to be substantially strong enough to sustain the loads applied by the actuators. The design effort and manufacturing cost of specimens for similar testing in the future can thus be greatly reduced without influencing the experimental accuracy. Verification tests of: (1) a symmetric specimen under uni-axial seismic excitation; (2) a mass-eccentric and stiffness-symmetric specimen under bi-axial seismic excitation have both been conducted. Satisfactory experimental results fully support the feasibility of the proposed bi-axial pseudodynamic technique as a powerful vehicle for future research on seismic performances of large scale three-dimensional structures.

ACKNOWLEDGMENT

The authors are grateful to acknowledge that this study was financially supported by the National Science Council, Taipei, Taiwan, R.O.C., under Grant No. NSC-88-2711-3-319-200-20.

REFERENCES

- Press, W. H., Teukolsky, S. A., Vetterling, W. T., and Flannery, B. P. (1992), *Numerical Recipes in Fortran*, 2nd ed., Cambridge University Press, New York.
- Thewalt, C.R. and Mahin, S.A. (1995), "Non-Planar Pseudodynamic Testing", *Earthquake Engineering and Structural Dynamics*, 24, pp733-746.

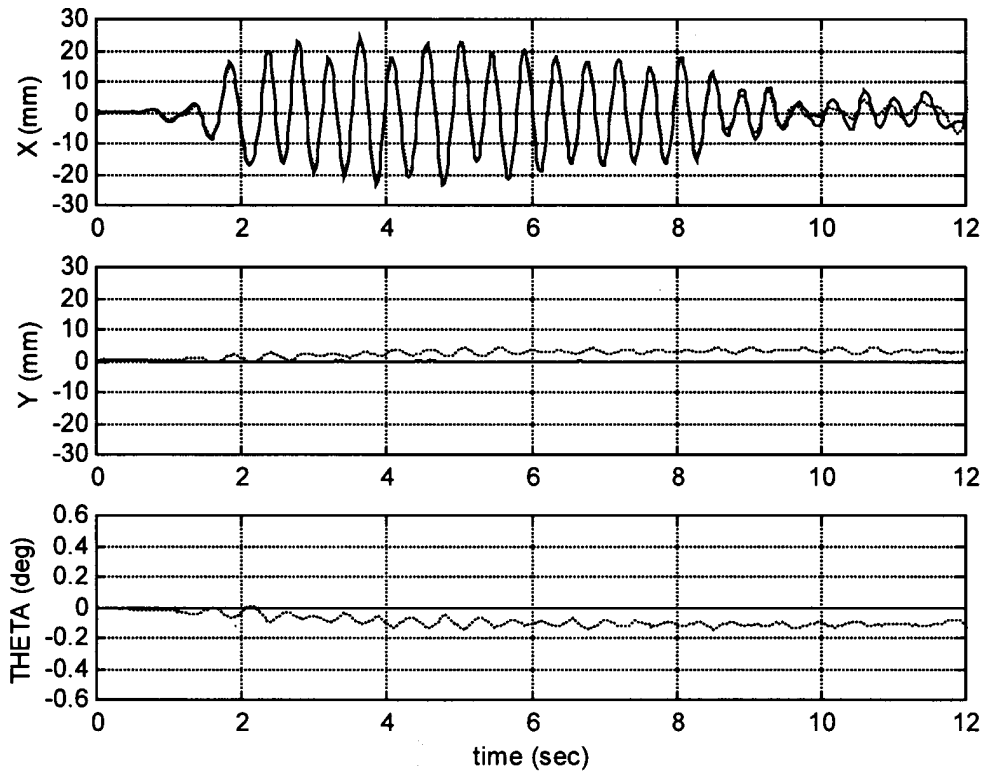


Figure 3. Response of the specimen (solid: pseudodynamic result; dotted: simulation).

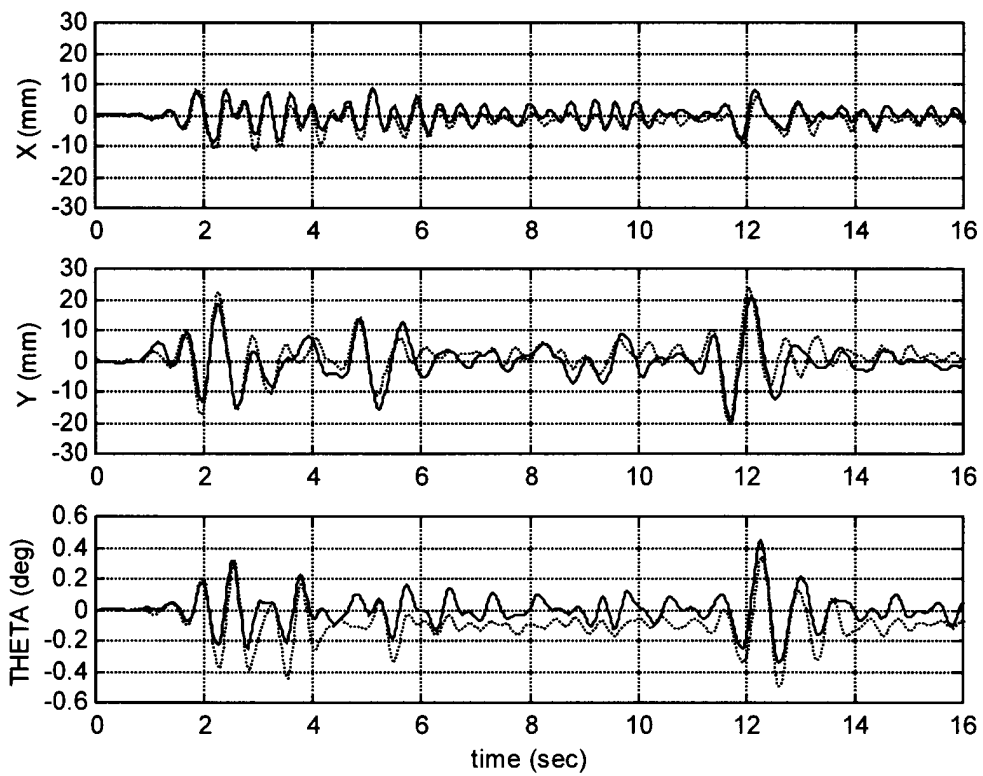


Figure 4. Response of the specimen (solid: pseudodynamic result; dotted: simulation).